Studies of Mossbauer spectra for nitrides $RTiFe_{11}N_x$ (R=Y, Nd, Sm, Gd and Er)

1992 J. Phys.: Condens. Matter 4 10409

(http://iopscience.iop.org/0953-8984/4/50/029)

J. Phys.: Condens. Matter 4 (1992) 10409–10420. Printed in the UK

Studies of Mössbauer spectra for nitrides $RTiFe_{11}N_x$ (R = Y, Nd, Sm, Gd and Er)

Z W Li, X Z Zhou and A H Morrish

Department of Physics, University of Manitoba, Winnipeg, Canada R3T 2N2

Received 28 July 1992

Abstract. Magnetic properties and ^{57}Fe Mössbauer spectra for the nitrides, $RTiFe_{11}N_x$, and for their parents $RTiFe_{11}$ (R = Y, Nd, Sm, Gd and Er) have been studied. The Curie temperatures of $RTiFe_{11}N_x$ increase by 135–200 °C over those for $RTiFe_{11}$. The maximum Curie temperature is 745 K for $GdTiFe_{11}N_x$. The Fe atomic moments at room temperature are 1.84 μ_B and 1.52 μ_B for $YTiFe_{11}N_x$ and $YTiFe_{11}$, respectively. Mössbauer spectra of the nitrides are fitted by using seven sets of subspectra, needed because the N atoms affect the hyperfine parameters. As compared to $RTiFe_{11}$, the average hyperfine field increases by 5–9 T and the average isomer shift by 0.10–0.18 mm s^{-1} for $RTiFe_{11}N_x$. For most of the $RTiFe_{11}$ series and their nitrides, the average hyperfine fields have a linear relationship with $(g_R - 1)J_R$, which can be understood with the RKKY theory. The core electron polarization field, B_{cp}, 4s electron polarization field, B_{4s}, and transfer field, B_{mp}, have been analysed and compared for the Y compound. The N atoms bring about an increase in magnitude of B_{cp} and B_{mp} and a decrease in magnitude of B_{4s}, which leads to an average increase of about 9 T in magnitude for the hyperfine field of $YTiFe_{11}N_x$ as compared to $YTiFe_{11}$. The proportionality coefficient between the average hyperfine field and the Fe moment for $YTiFe_{11}N_x$ deviates far from the normal value of 15 T μ_B^{-1}. This is attributed to a very large increase in the total conduction-electron polarization field.

1. Introduction

Recently, a series of interstitial nitrides $R_2Fe_{17}N_{3-x}$ has been prepared by using a gas–solid reaction [1,2]. The most striking feature of these new compounds is an increase of the Curie temperature by about 400 °C above that of the parent and a high uniaxial anisotropy with an anisotropy field of 14 T at room temperature for $Sm_2Fe_{17}N_{3-x}$. These excellent intrinsic magnetic properties have attracted much attention.

Later, another series of interstitial nitrides, $RTiFe_{11}N_x$, has been discovered [3,4]. These compounds have the same crystal structure as their parents, but the unit cell volume increases by about 1.2–3.0%. Their Curie temperatures increase by 60–140 °C. Most of the $RTiFe_{11}N_x$ compounds (R = Y, Nd, Gd, Dy, Ho, Tm and Lu) have a uniaxial anisotropy from 1.5 K to the Curie temperature. However, $SmTiFe_{11}N_x$ has a easy-plane anisotropy and $ErTiFe_{11}N_x$ has a spin reorientation at 45 K from a uniaxial to a cubic anisotropy. Among these nitrides, $NdTiFe_{11}N_x$ has an anisotropy field of 8 T and a saturation magnetization of 145 emu g^{-1} at room temperature and a Curie temperature of 740 K. It has the potential for use as a new permanent magnet material and can compete with $Sm_2Fe_{17}N_{3-x}$.

0953-8984/92/5010409+12$07.50

^{57}Fe Mössbauer spectra of $RTiFe_{11}$ have been studied [5–10]. Usually, there are two methods to fit the Mössbauer spectra. In one, the spectra are fitted by a sum of some separate subspectra, each corresponding to a certain crystallographic site. In the second, the spectra are fitted by using the binomial distribution method. [5,6] used four subspectra to fit the spectra of $YTi(Fe_{1-x}M_x)_{11}$ (M = Ni and Co) and [7] used five subspectra to fit the spectra of $RTiFe_{11}$. [8,9] considered the different nearest-neighbour coordinations of an Fe atom based on the random occupancy by the vanadium atoms on the 8i site in $RFe_{10}V_2$; the probability $P(n, m, x)$ of finding m nearest-neighbour vanadium atoms in a shell of n nearest-neighbour 8i atoms was calculated. These probabilities were used to obtain the relative intensities of the corresponding subspectra. However, the fit with a complicated distribution of hyperfine fields brought no significant improvement over a three-subspectrum fit [10].

$RTiFe_{11}N_x$ has a tetragonal structure with the space group $I4/mmm$, the same as $RTiFe_{11}$. The R atoms are located on the 2a site and the Fe atoms on the 8i, 8j and 8f sites. The Ti atoms only occupy the 8i site. The N atoms occupy the 2b site according to a neutron-diffraction experiment [11]. Figure 1 illustrates the tetragonal unit cell.

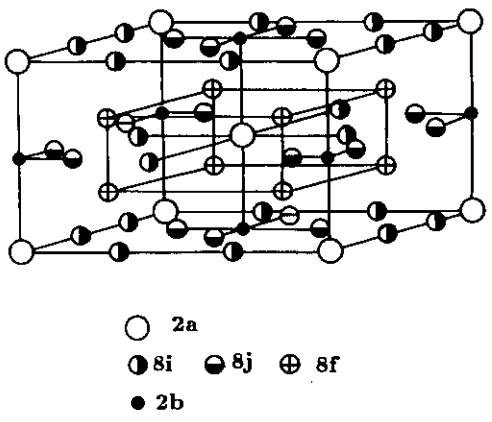

Figure 1. Schematic representation of the $ThMn_{12}$-type unit cell for $RTiFe_{11}N_x$.

In this work, Curie temperatures and saturation magnetizations have been measured and ^{57}Fe Mössbauer spectra have been collected and analysed for both the $RTiFe_{11}$ family (R = Y, Nd, Sm, Gd and Er) and their corresponding nitrides, $RTiFe_{11}N_x$, in an attempt to unravel the magnetic properties of these nitrides on an atomic scale.

2. Experimental details

$RTiFe_{11}$ (R = Y, Nd, Sm, Gd and Er) were prepared by arc-melting of better than 99.5% pure primary materials in a purified argon atmosphere followed by annealing at 1100–1200 K for 72 h in an argon atmosphere and then quenching in air. The $RTiFe_{11}$ compounds were ground to a fine powder (the size of the particles was smaller than 20 μm) and then heated in nitrogen at 2–3 atm. pressure at a temperature of 500 °C for 1 h.

X-ray diffraction experiments were performed with a diffractometer using Cu K_α radiation. Curie temperatures were obtained with a vibrating sample magnetometer in an applied field of 0.05 T. Magnetizations $M(H)$ were measured in applied fields up to 2 T at room temperature and saturation magnetizations were found by fitting experimental $M(H)$ against $1/H$ plots using the law of approach to saturation.

^{57}Fe Mössbauer spectra of the $RTiFe_{11}$ compounds, and their nitrides were taken at room temperature using a conventional constant-acceleration spectrometer. The γ-ray source was ^{57}Co in a Rh matrix. Mössbauer absorbers were powdered samples with about 8 mg cm^{-2} of natural iron. Calibration was made by using the spectrum of α-Fe at room temperature.

3. Results

3.1. X-ray and magnetic measurements

Within the limits of the x-ray diffractometer used, the $RTiFe_{11}$ compounds except R = Sm appeared to be single phase. A small amount of α-Fe was detected in $SmTiFe_{11}$ and all the $RTiFe_{11}N_x$ compounds. The lattice parameters for the $RTiFe_{11}$ family and their nitrides are listed in table 1. The nitrides, $RTiFe_{11}N_x$, retain their virginal $ThMn_{12}$ structure, but the lattice parameters, a and c, increase and the volume of the cell expands by about 3%. Meanwhile, the c/a ratio keeps the value of 0.560(5) in both virginal and nitrogenated $RTiFe_{11}$.

Table 1. Lattice parameters for $RTiFe_{11}$ and the corresponding nitrides.

	a (Å)	c (Å)	c/a	V (Å^3)	$\Delta V/V$ (%)
$YTiFe_{11}$	8.539	4.806	0.563	350	
$YTiFe_{11}N_x$	8.640	4.822	0.558	360	2.9
$NdTiFe_{11}$	8.625	4.814	0.558	358	
$NdTiFe_{11}N_x$	8.717	4.852	0.557	369	3.1
$SmTiFe_{11}$	8.577	4.797	0.559	353	
$SmTiFe_{11}N_x$	8.624	4.897	0.568	364	3.1
$GdTiFe_{11}$	8.547	4.802	0.562	351	
$GdTiFe_{11}N_x$	8.623	4.878	0.566	363	3.4
$ErTiFe_{11}$	8.504	4.795	0.564	347	
$ErTiFe_{11}N_x$	8.615	4.841	0.562	359	3.5

The Curie temperatures and saturation magnetizations for $RTiFe_{11}$ and their nitrides are listed in table 2. The Curie temperatures of the nitrides are raised by up to 135–200 °C over those for the $RTiFe_{11}$ parents. The highest Curie temperature is 745 K for $GdTiFe_{11}$ which is in accord with the $(g_R - 1)^2 J_R(J_R + 1)$ law. According to mean-field theory, if the R-R interaction is neglected, the Curie temperature in the rare-earth iron compounds can be expressed by

$$3kT_c = a_{FeFe} + (a_{FeFe}^2 + 4a_{FeR}a_{RFe})^{1/2} \tag{1}$$

where

$$a_{FeFe} = Z_{FeFe}J_{FeFe}S_{Fe}(S_{Fe} + 1)$$
$$a_{FeR}a_{RFe} = Z_{FeR}Z_{RFe}J_{FeR}^2 S_{Fe}(S_{Fe} + 1)(g_R - 1)^2 J_R(J_R + 1)$$

Table 2. Magnetic properties of $RTiFe_{11}$ and the corresponding nitrides. The specific magnetization σ_s, and the magnetization M_s refer to the room-temperature values. The figures in brackets indicate the experimental errors in the last significant digit.

	T_c K	σ_s (emu g^{-1})	M_s (μ_B FU^{-1})
$YTiFe_{11}$	525(5)	124(4)	16.7(6)
$YTiFe_{11}N_x$	713	149	20.2
$NdTiFe_{11}$	562	122	17.6
$NdTiFe_{11}N_x$	723	142	20.7
$SmTiFe_{11}$	593	121	17.6
$SmTiFe_{11}N_x$	742	138	20.3
$GdTiFe_{11}$	610	81	11.9
$GdTiFe_{11}N_x$	745	121	17.9
$ErTiFe_{11}$	518	84	12.5
$ErTiFe_{11}N_x$	718	125	18.7

In the above formulae, Z_{FeFe} represents the number of Fe neighbours to an Fe atom, Z_{FeR} the number of Fe neighbours to an R atom, Z_{RFe} the number of R neighbours to an Fe atom. Also J_{FeFe} and J_{FeR} are mean-field exchange coefficients and S_{Fe} and J_R are spin and angular momentum quantum numbers.

In $RTiFe_{11}$ and their nitrides, Z_{FeFe}, Z_{FeR} and Z_{RFe} are 9.9, 15 and 1.33 on average, respectively. If Z_{FeFe} together with the value $T_c = 713$ K for $YTiFe_{11}N_x$ and $S_{Fe} = 1$ are substituted into equation (1), $J_{FeFe} = 7.4 \times 10^{-22}$ J. For $GdTiFe_{11}N_x$, if this value of J_{FeFe} is used together with $T_c = 745$ K and $J_{Gd} = \frac{7}{2}$, then equation (1) yields the coupling constant $J_{GdFe} = 1.4 \times 10^{-22}$ J. By using the same method, the J_{FeFe} and J_{FeGd} are calculated to be 5.5×10^{-22} J and 2.1×10^{-22} J for $YTiFe_{11}$ and $GdTiFe_{11}$, respectively. Hence the Fe–Fe interaction is 35% higher for the nitride than for the parent and is clearly the source of the increased Curie temperature.

The saturation magnetizations, M_s, of $RTiFe_{11}$ and their nitrides at room temperature are also listed in table 2. From the results for Y compounds it can be shown that an N atom leads to a considerable increase in the Fe moment from 1.52 μ_B to 1.84 μ_B. The source would seem to be a redistribution in the up- and down-spins of the Fe 3d electrons produced by the interaction between the N 2p and Fe 3d electrons, hence leading to an increase in the Fe moment.

3.2. Mössbauer spectra

Since the quadrupole splitting was much smaller than the magnetic hyperfine-field splitting for all samples, a perturbation Hamiltonian was used to analyse the Mössbauer spectral data. The parameters obtained for each six-line pattern by a least-squares fitting procedure were the magnetic hyperfine field B_{hf} the quadrupole splitting ϵ, the isomer shift δ, the line widths and intensities. For almost all fits the relative areas for the six-lines of a subpattern were constrained to be in the ratio 3:2:1:1:2:3, respectively.

For simplicity, the Mössbauer spectra of $RTiFe_{11}$ (R = Y, Nd, Sm, Gd and Er) were fitted with three subpatterns, corresponding to the three Fe sites. Because the Ti atoms occupy only the 8i sites, the relative areas of the three subspectra were constrained to be in the ratio 3:4:4 for the 8i, 8j and 8f sites, respectively. The presence of the Ti introduced a distribution in the hyperfine parameters for each subpattern. Consequently, the use of only one six-line pattern for each site together with the constraint on the areas of the lines led to some, usually small, differences

in the line widths of corresponding pairs. For example, the line widths of the third and fourth lines for $ErTiFe_{11}$ are appreciably different. Besides $SmTiFe_{11}$, a small (about 1.1 %) α-Fe component was detected in $NdTiFe_{11}$; a subpattern for α-Fe was included in the fits to these two compounds. In addition, a paramagnetic doublet was introduced for $NdTiFe_{11}$. The spectral data and the computer fits for the $RTiFe_{11}$ samples are shown in figure 2; the Mössbauer parameters obtained are listed in table 3.

Table 3. Hyperfine parameters of $RTiFe_{11}$ at room temperature. Here B_{hf} is the hyperfine field, ϵ the quadrupole splitting and δ the isomer shift (relative to the α-Fe at room temperature).

	site	B_{hf} (T)	ϵ (mm s^{-1})	δ (mm s^{-1})	$\langle B_{hf} \rangle$ (T)
	8i	25.2(4)	0.27(2)	0.00(2)	
$YTiFe_{11}$	8j	23.0	−0.22	−0.32	23.1
	8f	21.6	0.28	−0.07	
	8i	26.8	0.19	−0.13	
$NdTiFe_{11}$	8j	20.5	−0.09	−0.30	22.0
	8f	19.9	0.30	−0.04	
	8i	28.9	0.12	−0.07	
$SmTiFe_{11}$	8j	25.6	−0.07	−0.36	26.3
	8f	25.1	0.11	−0.07	
	8i	28.2	0.10	−0.08	
$GdTiFe_{11}$	8j	25.0	−0.08	−0.30	25.4
	8f	23.6	0.24	−0.04	
	8i	25.8	0.08	−0.11	
$ErTiFe_{11}$	8j	23.1	−0.13	−0.36	23.7
	8f	22.7	0.06	−0.10	

For $RTiFe_{11}N_x$, a good fit with only three subspectra cannot be obtained. The effect of the N atoms on the hyperfine parameters must be considered. According to [11], N atoms occupy the 2b site and the value of x is about 0.5. This means that N atoms occupy only half of the 2b sites. The 8i and 8j sites have only one 2b site as their nearest-neighbour. Thus, there are two possible neighbour configurations for the Fe atoms; one has one N atom as a neighbour, the other has no N neighbour. Thus, each Mössbauer spectrum for the two sites should be split into two subspectra with an intensity ratio of 1:1. The 8f site has two 2b sites as its nearest-neighbours. There are three-neighbour configurations–two, one and zero N atoms with a probability of 0.25:0.5:0.25, respectively. Thus the spectrum for an 8f site should be split into three subspectra with an intensity ratio of 1:2:1. To summarize, the Mössbauer spectra of $RTiFe_{11}N_x$ are fitted with seven subspectra, whose relative areas are in the ratio 1.5:1.5:2:2:1:2:1.

To assign the subspectra to the corresponding Fe sites, we must consider the nearest-neighbour environments (table 4). For both $RTiFe_{11}$ compounds and their nitrides, the 8i site has the largest number of nearby neighbour Fe atoms (11.75 on average), whereas each 8j and 8f site has only nine adjacent Fe atoms. Thus, we believe that the largest hyperfine field should be for the 8i site. However, it is difficult to distinguish between the 8j and 8f site. According to most researchers' analyses and opinions, the hyperfine field on the 8j site is larger than that on the 8f site for the $RTiFe_{11}$ compounds [5–10]. Hence the magnitudes of the hyperfine fields have the sequences $B_{hf}(8i) > B_{hf}(8j) > B_{hf}(8f)$.

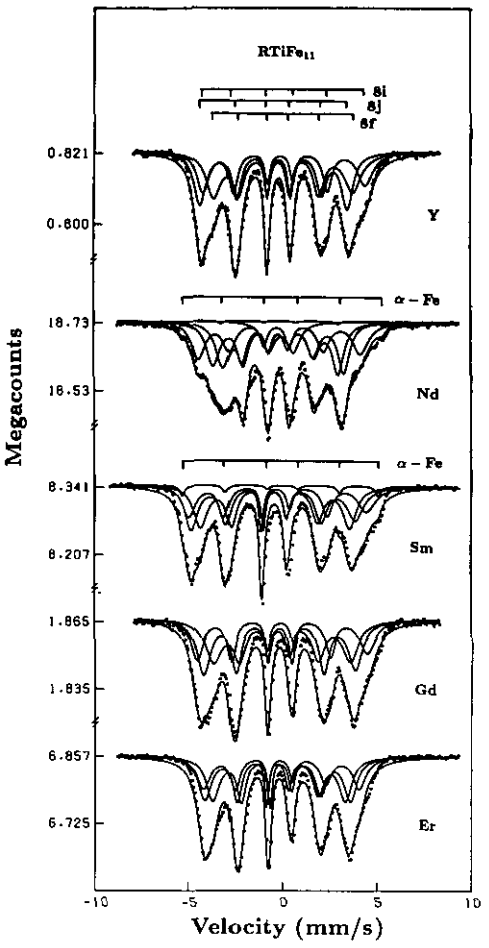

Figure 2. Mössbauer spectra and the computer-fitted curves for $RTiFe_{11}$.

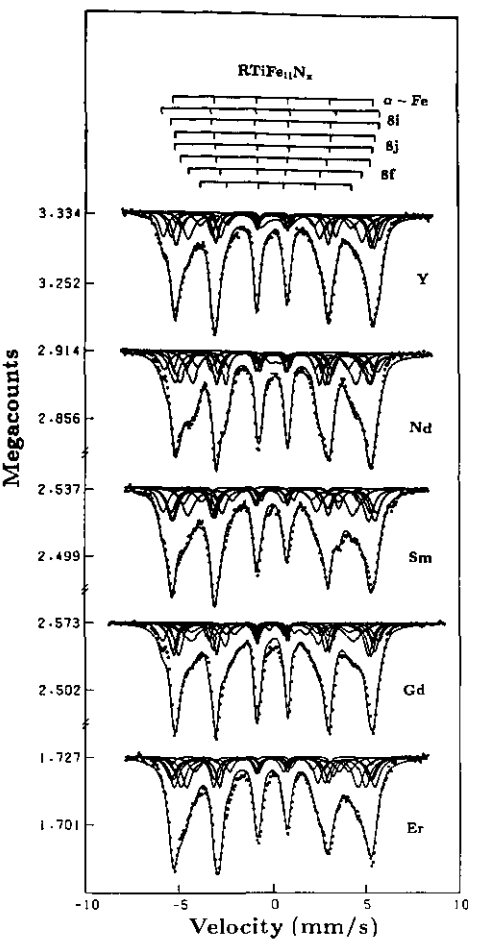

Figure 3. Mössbauer spectra and the computer-fitted curves for $RTiFe_{11}N_x$.

Table 4. Average interatomic distances (in Å) and the numbers of adjacent atoms for each site in $YTiFe_{11}N_x$ (values in the bracket are for $YTiFe_{11}$).

Site	d_{Fe-Fe} (Å)	d_{Fe-Y} (Å)	d_{Fe-N} (Å)	$n_{Fe-Fe} + n_{Fe-R} + n_{Fe-N}$
8i	2.777(2.712)	2.950(3.104)	3.809	13+1+1
8j	2.607(2.594)	3.089(3.058)	1.932	10+2+1
8f	2.510(2.518)	3.274(3.265)	3.274	10+2+2

During the fitting, a small amount (3-5% of total absorption) of an α-Fe spectrum was included for all the nitrides. In addition, a weak central paramagnetic doublet (<3% of total absorption) was introduced for some of the spectra. The Mössbauer spectra and the subpatterns for the $RTiFe_{11}N_x$ samples are shown in figure 3. The associated parameters obtained are listed in table 5.

The hyperfine fields on each site for each $RTiFe_{11}$ and their corresponding nitrides are plotted in figure 4. For $RTiFe_{11}$, the hyperfine fields on the 8i site are about 3

Table 5. Hyperfine parameters of $RTiFe_{11}N_x$ at room temperature. Here B_{hf} is the hyperfine field, ϵ is the quadrupole splitting and δ is the isomer shift (relative to the α-Fe at room temperature).

	site	B_{hf} (T)	ϵ (mm s^{-1})	δ (mm s^{-1})	$\langle B_{hf} \rangle$ (T)
	8i	35.5(4)	0.05(2)	−0.01(2)	
$YTiFe_{11}N_x$	8j	32.8	0.14	0.00	32.0
	8f	28.7	0.26	−0.05	
	8i	34.0	−0.07	0.03	
$NdTiFe_{11}N_x$	8j	32.1	0.09	−0.01	30.8
	8f	27.2	0.05	0.05	
	8i	34.4	−0.21	−0.02	
$SmTiFe_{11}N_x$	8j	32.8	0.05	−0.04	31.1
	8f	26.9	0.02	−0.09	
	8i	34.8	−0.06	−0.08	
$GdTiFe_{11}N_x$	8j	32.6	0.06	−0.04	31.4
	8f	27.7	−0.00	−0.05	
	8i	33.2	−0.08	−0.04	
$ErTiFe_{11}N_x$	8j	32.1	0.13	−0.01	30.7
	8f	27.6	−0.11	−0.18	

and 4 T larger than those on the 8j site and 8f sites, respectively, except for $NdTiFe_{11}$. On the other hand, the fields on the 8j site are only 0.5–1.4 T larger than those on the 8f site. For $RTiFe_{11}N_x$ as compared to $RTiFe_{11}$, the hyperfine fields increase by about 5–9 T on average and by 5.5–10 T, 7.2–11.6 T and 1.8–7.3 T for the 8i, 8j and 8f sites, respectively.

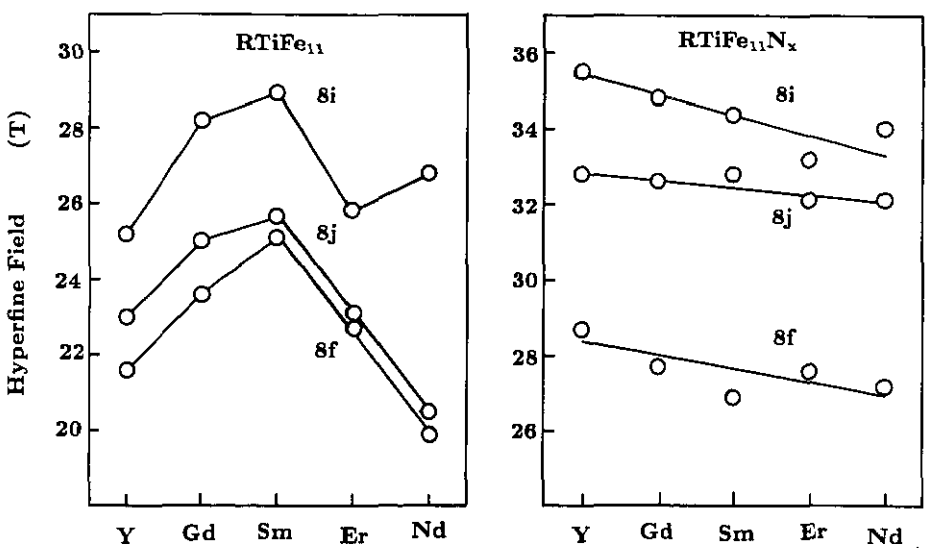

Figure 4. Hyperfine fields B_{hf} on the three iron sites of $RTiFe_{11}$ and $RTiFe_{11}N_x$.

As compared to $RTiFe_{11}$, there is an increase of 0.10–0.18 mm s^{-1} in the average isomer shift of the nitrides. The isomer shift for the 8j site has the largest increase (about 0.30 mm s^{-1}), as expected, because this site is closest to the N atom. Specifically, this distance of 1.9 Å is much shorter than the distances (about 3.8 and

3.3 Å) of the other two sites to an N atom. The isomer shifts on the 8i and 8f sites are either slightly increased or are unchanged for all nitrides. There are two factors which are largely responsible for the increase in the isomer shift for the nitrides. One is expansion of the cell volume for the nitrides. Since the cell volume expands about 3% compared to the $RTiFe_{11}$ compounds, and the relationship between the isomer shift and volume is given by $\Delta\delta/(\Delta V/V) = 1.33\,\mathrm{mm\,s^{-1}}$ for α-Fe [12], the contribution of the volume expansion to the isomer shift is estimated to be 0.04–0.05 $\mathrm{mm\,s^{-1}}$, as shown in table 6. The other is the transfer of electrons in nitrides. Since the electronegativity is much larger for N than for Fe, the N atoms have a tendency to attract the conduction electrons of Fe. A decrease in the Fe conduction electrons will cause an increase in the isomer shift.

Table 6. Average isomer shift for $RTiFe_{11}$ and $RTiFe_{11}N_x$ as well as the increase of isomer shift caused by expansion of the cell volume. δ^* and δ^{**} are the average isomer shift for $YTiFe_{11}$ and $YTiFe_{11}N_x$, respectively. $\Delta\delta^a$ is the difference between δ^{**} and δ^*. $\Delta\delta^V$ is an increase of isomer shift from expansion of the cell volume.

	δ^* ($\mathrm{mm\,s^{-1}}$)	δ^{**} ($\mathrm{mm\,s^{-1}}$)	$\Delta\delta^a$ ($\mathrm{mm\,s^{-1}}$)	$\Delta V/V$ (%)	$\Delta\delta^V$ ($\mathrm{mm\,s^{-1}}$)
Y	−0.14	−0.02	0.12	2.9	0.04
Nd	−0.16	0.02	0.18	3.1	0.04
Sm	−0.18	−0.05	0.13	3.1	0.04
Gd	−0.15	−0.05	0.10	3.4	0.05
Er	−0.20	−0.08	0.12	3.5	0.05

4. Discussion

4.1. 3d Magnetic Properties

It is known that the hyperfine field consists of three parts, a Fermi contact field B_c, an orbital field B_{orb} and a dipolar field B_{dip}. The dipolar field will be neglected because it is small in metals. The Fermi contact field is usually divided into three parts. One is the core-electron (1s, 2s and 3s electrons) polarization field B_{cp}, which has a negative sign. The other two are conduction-electron polarization fields. One is produced by the Fe 3d moment itself, is called the 4s polarization field B_{4s}, and always has a positive sign. The other polarization field is produced by the moment of the adjacent Fe atoms, is called the transfer field B_{mp}, and has either a negative or a positive sign. Thus, the hyperfine field B_{hf}, in $YTiFe_{11}$ or $YTiFe_{11}N_x$, can be expressed as

$$B_{hf} = B_{cp} + B_{4s} + B_{mp} + B_{orb}. \tag{2}$$

Both B_{cp} and B_{4s} are proportional to the moment of the Fe atom on the site. B_{mp} is proportional to the moment and the number of adjacent Fe atoms. For example, $B_{cp}(k)$, $B_{4s}(k)$ and $B_{mp}(k)$ on the kth site, where $k = 1$, 2 or 3 represent the 8i, 8j or 8f sites respectively, are given by

$$B_{cp}(k) = a\mu_{Fe}(k) \tag{3}$$

$$B_{4s}(k) = b\mu_{Fe}(k) \tag{4}$$

$$B_{mp}(k) = c\sum_{m=1}^{3} n_{Fe}(m)\mu_{Fe}(m) \tag{5}$$

where $\mu_{Fe}(k)$ is the Fe moment on the kth site, $\mu_{Fe}(m)$ and $n_{Fe}(m)$ are the moments and numbers of the Fe atoms on the mth site arounding the kth site, where $m = 1$, 2, or 3 represents the 8i, 8j, or 8f site, and a, b and c are hyperfine coupling constants. For a given site in a given material a, b, and c are constants; however $a \neq b \neq c$. If $\mu_{Fe}(m)$ in equation (5) is replaced by an average moment $\overline{\mu_{Fe}}$ and $n_{Fe}(k) = \sum_{m=1}^{3} n_{Fe}(m)$ is the number of adjacent Fe atoms surrounding the kth site, equation (5) can be written as

$$B_{mp}(k) = c \sum_{m=1}^{3} n_{Fe}(m)\mu_{Fe}(m) = cn_{Fe}(k)\overline{\mu_{Fe}}. \tag{6}$$

Hence $B_{hf}(k)$ is given by

$$B_{hf}(k) = a\mu_{Fe}(k) + b\mu_{Fe}(k) + cn_{Fe}(k)\overline{\mu_{Fe}} + B_{orb}. \tag{7}$$

First, we estimate the magnitude of the orbital field. A calculation for α-Fe shows that the orbital moment is 0.09 μ_B [13] and the orbital field is about 2.5 T [14]. Thus, a proportionality coefficient of 28 T μ_B^{-1} is obtained. In R-Fe compounds the orbital moment of Fe is usually small, 0.02 μ_B for Y_2Fe_{17} [15], 0.05 μ_B for $Nd_2Fe_{14}B$ [15] and 0.07 μ_B for $LuFe_2$ [16] as obtained either by calculation or in polarized neutron-diffraction experiments. If an average value 0.05 μ_B is taken as the orbital moment of $YTiFe_{11}$ and $YTiFe_{11}N_x$, the orbital field obtained is 1.4 T. Now it is assumed that the orbital fields are constants for the three sites in $YTiFe_{11}$ and its nitride. As the orbital field is small and only 4–7% of the total hyperfine field, this approximation does not significantly affect the following calculation. Second, the core-electron polarization field is proportional to the Fe moment with a proportionality constant of $-11.3\,T\ \mu_B^{-1}$ [17, 18]. The Fe moment for the three sites can be obtained from neutron-diffraction experiments [19, 11] (as listed in table 7). Thus, the field $B_{cp}(k)$ can be calculated from equation (3). In equation (7) $n_{Fe}(k)$ was taken to be 11.75, 9 and 9 for the 8i, 8j and 8f sites, respectively. Then, on substituting for $B_{cp}(k)$, $B_{orb}(k)$ and $B_{hf}(k)$ in equation (7) and solving the equation sets by using the least-squares method, the hyperfine coupling constants b and c are calculated to be $b = 4.66$ and $c = -0.97\,T\ \mu_B^{-1}$ for $YTiFe_{11}$ and $b = 2.07$ and $c = -0.93\,T\ \mu_B^{-1}$ for $YTiFe_{11}N_x$. Finally, on substituting b and c into equations (4) and (6) the 4s polarization and transfer fields are obtained. The calculated B_{cp}, B_{4s}, B_{mp} and $B_{hf}^{cal.}$ values are listed in table 7. The calculated $B_{hf}^{cal.}$ are very consistent with the results obtained from the Mössbauer spectra.

Compared to $YTiFe_{11}$, there is an increase of 8.9 T on the average in the magnitude of the hyperfine field for $YTiFe_{11}N_x$. This increase is attributed to three factors. (i) The magnitude of the core-electron polarization field, B_{cp}, increases by 3.6 T, which has its source in the increase of the Fe moment. (ii) The magnitude of the 4s polarization field B_{4s}, decreases by 3.3 T. It is known that the electronegativity is 3.09 for an N atom and 1.64 for an Fe atom. Thus the N atoms tend to attract conduction electrons from the Fe atoms. The electron-band calculations for the cubic γ-phase Fe_4N also show that there exists a strong interaction between N 2p and Fe 4s orbitals. This interaction leads to an transfer from the Fe 4s electrons to the N 2p electrons [20, 21]. In addition, an increase of 0.12 mm s^{-1} in the isomer shift for $YTiFe_{11}N_x$ indicates a decrease in the number of Fe 4s electrons. These

Table 7. Hyperfine fields for $YTiFe_{11}$ and $YTiFe_{11}N_x$. B_{cp} is the core-electron polarization field; B_{4s} is the 4s electron polarization field of the Fe moment itself and B_{mp} is the transfer field. The Fe moments are taken from [19, 11].

Site	μ_{Fe} (μ_B)	B_{cp} (T)	B_{4s} (T)	B_{mp} (T)	B_{orb} (T)	$B_{hf}^{cal.}$ (T)	$B_{hf}^{exp.}$ (T)
$YTiFe_{11}$							
8i	1.45	−16.4	6.8	−17.3	1.4	−25.5	−25.2
8j	1.73	−19.5	8.1	−13.2	1.4	−23.2	−23.0
8f	1.36	−15.4	6.3	−13.2	1.4	−20.9	−21.6
Average	1.52	−17.2	7.1	−14.3	1.4	−23.0	−23.1
$YTiFe_{11}N_x$							
8i	1.72	−19.4	3.6	−20.1	1.4	−34.5	−35.5
8j	2.12	−24.0	4.4	−15.4	1.4	−33.6	−32.8
8f	1.69	−18.6	3.4	−15.4	1.4	−29.2	−28.7
Average	1.84	−20.8	3.8	−16.7	1.4	−32.2	−32.0

results show that N atoms bring about a decrease in the number of 4s conduction electrons and therefore leads to a decrease in the magnitude of the 4s-polarization field, since the coupling constant b depends on the number of 4s spins contributing to the polarization and on the strength of the exchange interaction between the 4s and 3d electrons [22]. (iii) The magnitude of the transfer field B_{mp}, increases by 2.4 T. The coupling constant c has almost same value for $YTiFe_{11}$ and $YTiFe_{11}N_x$. So the increase in magnitude of the transfer field can be attributed to the increase in the Fe moment.

In addition, it is known that the average hyperfine field is proportional to the average Fe moment; a coefficient of 15 T μ_B^{-1} has been obtained from experiments on Y–Fe systems [6,23]. This rule is also applicable to $YTiFe_{11}$. However, in $YTiFe_{11}N_x$, the average Fe moment is 1.84 μ_B and the average hyperfine field is 32.0 T. The proportionality coefficient is 17.4 T μ_B^{-1}, which is far from the normal value of 15 T μ_B^{-1}. From table 7, average Fe moments are 1.52 μ_B and 1.84 μ_B for $YTiFe_{11}$ and $YTiFe_{11}N_x$, respectively; in other words, the average Fe moment increases by 21% for the nitride. In spite of an increase of 21% in the core-electron polarization field, the total conduction electron polarization fields, $B_{4s} + B_{mp}$, are 12.9 T and 7.2 T for $YTiFe_{11}N_x$ and $YTiFe_{11}$, respectively, an increase of about 80%. The very large contribution by the conduction electrons produces a total hyperfine field, B_{hf}, increase of 39%, which is much more than the increase, 21%, in the average Fe moment. Consequently, the proportionality coefficient between the average hyperfine field and the average Fe moment is larger for $YTiFe_{11}N_x$ than for $YTiFe_{11}$.

4.2. R-atom magnetic properties

The hyperfine fields averaged over the three sites as plotted against $(g_R - 1)J_R$ for both $RTiFe_{11}$ and $RTiFe_{11}N_x$ are shown in figure 5. It is seen that the dependence is linear to a good approximation. Since R atoms have magnetic moments, the transferred field comes not only from Fe atoms (B_{mp}), but also from R atoms (B_{rp}). Thus B_{rp} has to be introduced into equation (2),

$$B_{hf} = B_{cp} + B_{orb} + B_{4s} + B_{mp} + B_{rp} \tag{8}$$

$$B_{hf} = B_{Fe} + B_{rp} \tag{9}$$

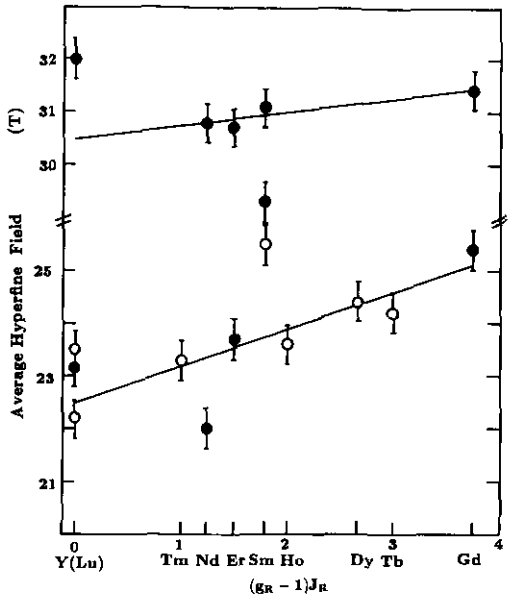

Figure 5. Average hyperfine fields $\langle B_{hf} \rangle$ for $RTiFe_{11}$ and $RTiFe_{11}N_x$ versus $(g_R - 1)J_R$. (Data with open circles are taken from Hu *et al* [7].)

The first four terms are related to the Fe moments. They are written as B_{Fe} and can approximately be considered to be a constant for $RTiFe_{11}$ compounds and a different constant for the nitrides (R = Y, Nd, Sm, Gd and Er). The last term is the transfer field produced by the R moments. It is most conveniently expressed in term of the RKKY theory where B_{rp} is proportional to $(g_R - 1)J_R \sum_i F(2k_F r_i)$. The summation $\sum_i$ extends over all distances r_i between the central Fe nucleus considered and the R atoms of the lattice. The function $F(2k_F r)$ is the RKKY function and k_F is wave number at the Fermi surface. For a given series of isostructural compounds the function $\sum_i F(2k_F r_i)$ can be considered to be a constant so that B_{rp} is proportional to $(g_R - 1)J_R$. Thus, equation (9) can be rewritten as

$$B_{hf} = B_{Fe} + \alpha(g_R - 1)J_R \tag{10}$$

By applying the least-squares method to equation (10), $B_{Fe} = 22.5(3)$ T and $\alpha = 0.70(12)$ for $RTiFe_{11}$, and $B_{Fe} = 30.5(2)$ T and $\alpha = 0.25(7)$ for $RTiFe_{11}N_x$.

From figure 5 it follows that:

(i) The contributions of the Fe atoms to the hyperfine field are 22.5 and 30.5T for the series of $RTiFe_{11}$ and $RTiFe_{11}N_x$ compounds, respectively. They are slightly smaller than the 23.1 and 32.0 T obtained for $YTiFe_{11}$ and $YTiFe_{11}N_x$, respectively.

(ii) The transfer field B_{rp} produced by the R atoms is smaller for $RTiFe_{11}N_x$ than for $RTiFe_{11}$.

(iii) The hyperfine fields of $SmTiFe_{11}$ and $NdTiFe_{11}$ have larger deviations from a linear relationship between the hyperfine field and $(g_R - 1)J_R$. This abnormality also exists for RV_2Fe_{10} where the hyperfine field of SmV_2Fe_{10} is larger than that of GdV_2Fe_{10}; the origin may be compositional deviations during the arc melting [8].

5. Conclusions

(i) The Curie temperatures are 135–200°C higher for a $RTiFe_{11}N_x$ compound than for the corresponding $RTiFe_{11}$ composition (R = Y, Nd, Sm, Gd and Er). The maximum Curie temperature is 745 K for $GdTiFe_{11}N_x$. The Fe moments at room temperature are 1.52 μ_B and 1.84 μ_B for $YTiFe_{11}$ and $YTiFe_{11}N_x$, respectively.

(ii) As compared to $RTiFe_{11}$, the average hyperfine field increases by 5–9 T and the average isomer shift by 0.10–0.18 mm s^{-1} for $RTiFe_{11}N_x$.

(iii) The N atoms bring about an increase in magnitude of B_{cp} and B_{mp} and a decrease in magnitude of B_{4s}, which leads to an increase of about 9 T in magnitude of the hyperfine field for $YTiFe_{11}N_x$ as compared to $YTiFe_{11}$.

(iv) The proportionality coefficient between the average hyperfine field and the Fe moment for $YTiFe_{11}N_x$ is larger than the normal value 15 T μ_B^{-1}; this is attributed to a very large increase in the total conduction-electron polarization field.

(v) For most $RTiFe_{11}$ compounds and their nitrides, the average hyperfine field has a linear relationship with $(g_R - 1)J_R$, a result that can be understood with the RKKY theory.

References

[1] Coey J M D and Sun Hong 1990 *J. Magn. Magn. Mater.* **87** L251
[2] Sun Hong, Otani Y, Hurley D P F and Coey J M D 1990 *J. Phys. : Condens. Matter* **2** 6465.
[3] Yang Y C, Zhang X D, Kong L S, Pan Q and Ge S L 1991 *Solid State Commun.* **78** 317
[4] Yang Y C, Zhang X D, Ge S L, Kong L S, Pan Q, Yang J L, Zhang B S, Ding Y F and Ye C T 1991 *J. Appl. Phys.* **70** 6001
[5] Li Z W, Zhou X Z, Morrish A H and Yang Y C 1990 *J. Phys.: Condens. Matter* **2** 4253
[6] Li Z W, Zhou X Z, Morrish A H and Yang Y C 1990 *J. Phys.: Condens. Matter* **2** 9621
[7] Hu Bo-Ping, Li Hong-Shuo, Gavigan J P and Coey J M D 1989 *J. Phys. : Condens. Matter* **1** 755
[8] Sinnemann Th, Rosenberg M and Buschow K H J 1989 *J. Less-Common Met.* **146** 223
[9] Denissen C J M, Coehoorn R and Buschow K H J 1990 *J. Magn. Magn. Mater.* **87** 51
[10] Sinnemann Th, Wisniewski M-U, Rosenberg M and Buschow K H J 1989 *J. Magn. Magn. Mater.* **83** 259
[11] Yang Y C, Zhang X D, Kong L S, Pan Q, Ge S L, Yang J L, Ding Y F, Zhang B S, Ye C T and Jin L 1991 *Solid State Commun.* **78** 313
[12] Williamson D L, Bukshpan S and Ingalls R 1972 *Phys. Rev.* B **6** 4194
[13] Reck R A and Fry D L 1969 *Phys. Rev.* **184** 492
[14] Stearns M B 1987 *Landolt-Börnstein, New Series Group III* vol 19a (Berlin: Springer) ed Hellwege K H and Madelung O
[15] Szpunar B, Wallace W E and Szpunar J 1987 *Phys. Rev.* B **36** 3782
[16] Givord D, Gregory A R and Schweizer J 1980 *J. Magn. Magn. Mater.* **15-18** 293
[17] Coehoorn R, Denissen C J M and Eppenga R 1991 *J. Appl. Phys.* **69** 6222
[18] Beuevle T and Fähule M 1992 *J. Magn. Magn. Mater.* **110** L29
[19] Yang Y C, Sun H, Kong L S, Yang J L, Ding Y F, Ye B S, Jin L and Zhou H M 1988 *J. Appl. Phys.* **64** 5968.
[20] Zhou Wei, Qu Li-jia, Zhang Qi-ming and Wang Ding-sheng 1989 *Phys Rev.* B **40** 6393
[21] Sakuma A 1991 *J. Phys. Soc. Japan* **60** 2007
[22] Niculescu V A, Burch T J and Budnick J I 1983 *J. Magn. Magn. Mater.* **39** 223
[23] Gubbens P C M, Van Apeldoorn J H F, Van der Kraan A M and Buschow K H J 1974 *J. Phys. F: Met. Phys.* **4** 921